Spatial distribution of the absolute densities of CF_x radicals in fluorocarbon plasmas determined from single-path infrared laser absorption and laser-induced fluorescence

Masayuki Nakamura, Masaru Hori,[a] and Toshio Goto
Department of Quantum Engineering, School of Engineering, Nagoya University, Furo-cho, Chikusa-ku, Nagoya 464-8603, Japan

Masafumi Ito
Department of Opto-Mechatronics Faculty of Systems Engineering, Wakayama University, 930 Sakaedani, Wakayama 640-8510, Japan

Nobuo Ishii
Central Research Laboratory, Tokyo Electron Ltd., 4-1-14 Miyahara, Yodogawa-ku, Osaka 532-0003, Japan

(Received 22 March 2000; accepted for publication 8 November 2000)

The spatial distribution of the absolute density of CF_x ($x=1-3$) radicals and their translational temperatures in an electron cyclotron resonance (ECR) plasma generated from a tetrafluorocarbon (C_4F_8) gas were examined using infrared diode-laser absorption spectroscopy (IRLAS) without a multiple reflection cell, namely, single-path IRLAS. Furthermore, we have developed a method of measuring CF and CF_2 radical densities using single-path IRLAS combined with laser-induced fluorescence (LIF) spectroscopy. This method enables us to measure the spatial distribution of absolute radical densities with high accuracy, because of the IRLAS infrared laser beam and the LIF ultraviolet laser beam having identical paths. Under all the conditions studied, a spatially hollow distribution of the CF_2 radical density is formed; the CF_2 radical density in the vicinity of the chamber wall is much higher than that in the plasma. However, the spatial distribution of the CF radical density differs greatly from that of the CF_2 radical density. The translational temperatures of CF and CF_2 radicals are evaluated to be ~700 K. On the basis of the measured results, we clarify the mechanisms of the formation of the spatial distribution, and conclude that the hollow distribution of the CF_2 radical density is not caused by radical generation from the chamber wall, rather, the dominant mechanism for the formation of this distribution is the electron-impact dissociation of C_4F_8 gas in the ECR region and diffusion from the upper part of the plasma chamber under the present plasma conditions where the flux of ions incident to the chamber wall is low.
 [DOI: 10.1063/1.1337090]

I. INTRODUCTION

As the integration density of ultralarge scale integrated circuits (ULSIs) increases and chip sizes shrink, multilevel interconnection technology is becoming increasingly important. However, the high parasitic capacitance of interconnections limits the signal transmission rate of devices and is becoming a serious problem. The reduction of parasitic capacitance is therefore indispensable to improving signal transmission rates. One of the most effective ways to reduce parasitic capacitance is to use low dielectric materials as interlayer dielectrics. Many techniques of synthesizing low dielectric constant films have been investigated, in particular, fluorinated carbon films have been formed by plasma processes employing fluorocarbon gases.[1] The fluorocarbon plasma process has also been used in the selective etching of silicon oxide on silicon and silicon nitride layers for fabricating contact holes in ULSIs. It has been found that etching selectivity occurs due to the selective formation of protective fluorocarbon films on the underlying silicon and silicon nitride.

The growth mechanism of these fluorocarbon films, however, has not yet been sufficiently clarified. It is considered that neutral fluorocarbon radicals play a very important role in film formation. Therefore, the measurement of the absolute density of radicals in the plasma is necessary in order to clarify the growth mechanism of these films.

Moreover, as wafers become larger, approaching 12 in. in diameter, low-dielectric film formation and etching processes that are uniform over the entire area of large wafers are strongly requested. Fluorocarbon films deposited on the wall of a plasma reactor change the conditions of the chamber wall, considerably influencing the sticking coefficient of radicals to the wall and resulting in changes in radical densities in the plasma.[2] These changes affect not only the uniformity of the films deposited on the substrate, but also the repeatability of the processes. Therefore, measurement of the spatial distribution of absolute radical densities in the plasma reactor and the clarification of the formation mechanisms are

[a]Electronic mail: hori@nuee.nagoya-u.ac.jp

indispensable to achieving the high performance plasma processing.

Laser-induced fluorescence (LIF) spectroscopy has been used extensively to investigate the spatial distributions of CF and CF_2 radicals in fluorocarbon plasmas.[3] LIF measurements have high sensitivity and high spatial resolution. It is, however, impossible to derive the absolute densities of CF and CF_2 radicals directly without calibration. In the past, calibration procedures have involved Rayleigh scattering or ultraviolet absorption spectroscopy, and relative densities obtained by LIF measurements have been transformed to absolute values. These techniques have inherent difficulties in calibrating the densities accurately because of the differing sampling volumes for LIF measurement and other measurements employed for calibration.

We have established a method of measuring absolute CF_x ($x=1-3$) radical densities using infrared diode-laser absorption spectroscopy (IRLAS),[4] and we have clarified the behavior of radicals in high-density electron cyclotron resonance (ECR) plasmas with fluorocarbon gases.[2,5,6] To date, a multiple reflection cell has commonly been used in IRLAS to improve the sensitivity of the technique. To measure the spatial distribution of radical densities in the plasma reactor, we have developed an IRLAS method that employs a single beam path, namely, single-path IRLAS. Furthermore, we have developed a method of measuring CF and CF_2 radical densities using single-path IRLAS combined with a LIF spectroscopy. Using this method, it is possible to obtain the spatial distribution of absolute density with high accuracy.

In this study, we measured the spatial distributions of the absolute density and translational temperatures of CF_x radicals in C_4F_8 gas ECR plasmas by single-path IRLAS. Then, by combining single-path IRLAS with LIF, we measured the precise spatial distributions of the absolute densities of CF and CF_2 radicals in the plasmas. On the basis of the measured results, we discuss the mechanism of the spatial distribution formation of radicals in the plasma reactor.

II. EXPERIMENT

A schematic diagram of the ECR plasma reactor with single-path IRLAS and LIF measurement systems used in this study is shown in Fig. 1. The plasma chamber was rectangular parallelepiped, with a long axis of 54 cm for laser pass direction, as specially designed for the single-path IRLAS and LIF measurements. An 8 in. Si wafer was placed on the substrate holder. A continuous 2.45 GHz microwave was introduced into the plasma reactor at the top of the reactor. The mirror-type magnetic field was formed by a main and two submagnet coils, and the ECR plasma was confined within a region 25 cm in diameter and 19 cm in height on the substrate. C_4F_8 gas was injected into the plasma chamber through a ring-shaped nozzle. The nozzle was inclined from horizontal by 10°. The ring was made from a 2.8 cm diameter stainless steel pipe fabricated in a ring 39 cm in diameter and set 7.5 cm above the substrate. The ECR region of 875 G was located at about 14 cm above the substrate. The substrate was heated at 170 °C and the chamber wall was maintained at 80 °C.

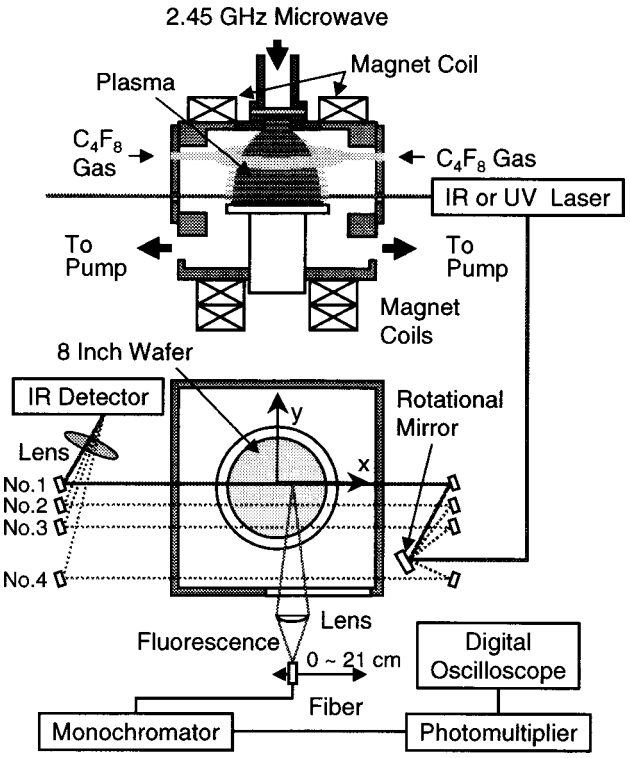

FIG. 1. Schematic diagram of ECR plasma reactor and radical measurement systems with single-pass IRLAS and LIF measurement systems.

The guiding laser system consisted of eight small fixed mirrors and a rotational mirror. An infrared or ultraviolet laser beam was first reflected by the rotational mirror. By rotating the mirror, the laser beam was directed to one of the fixed mirrors, thereby passing through the plasma chamber 1 cm above the substrate. The diameter of both laser beams was about 3 mm. The location of the beam path could be varied anywhere from the center of the chamber to the vicinity of the chamber wall. The laser beam reflected by mirror 3 passed directly above the edge of the wafer. The beam reflected by mirrors 1, 2, and 3 all passed through the plasma region, whereas the beam reflected by mirror 4 passed outside the plasma region.

In IRLAS measurement, absolute radical densities were obtained as line-averages. In LIF measurement, by moving the fluorescence detector parallel to the No. 1 laser beam path, the precise spatial distribution of relative radical densities could be determined. The absorption lines used for IRLAS in this study were the ${}^{Q}R_4(26)$ line of the CF_2 band at 1132.7532 cm^{-1}, the $R_2(7.5)$ line of the CF band at 1308.6702 cm^{-1}, and the ${}^{R}R_{18}(18)$ line of the CF_3 band at 1262.1039 cm^{-1}. The procedure for calculating radical densities are described in detail elsewhere.[7] The translational temperatures were calculated from the full width at half maximum of each spectral profile. In this study, the translational temperature of CF radicals was calculated in full consideration of the Zeeman effect because the spectra of the CF radicals were broadened due to the magnetic field. For LIF measurement, the excitation wavelengths of CF and CF_2 radicals are 232.66 $[A^2\Sigma^+(v'=0)\leftarrow X^2\Pi(v''=0)]$ and 261.7 $[\tilde{A}(0,2,0)\leftarrow\tilde{X}(0,0,0)]$ nm, respectively,[8] and the fluo-

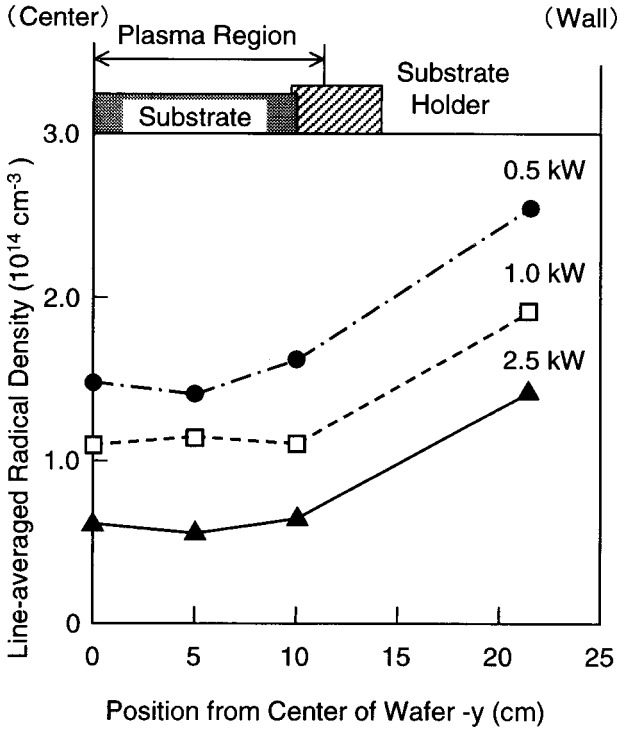

FIG. 2. Spatial distribution of absolute CF_2 radical density as a function of microwave power.

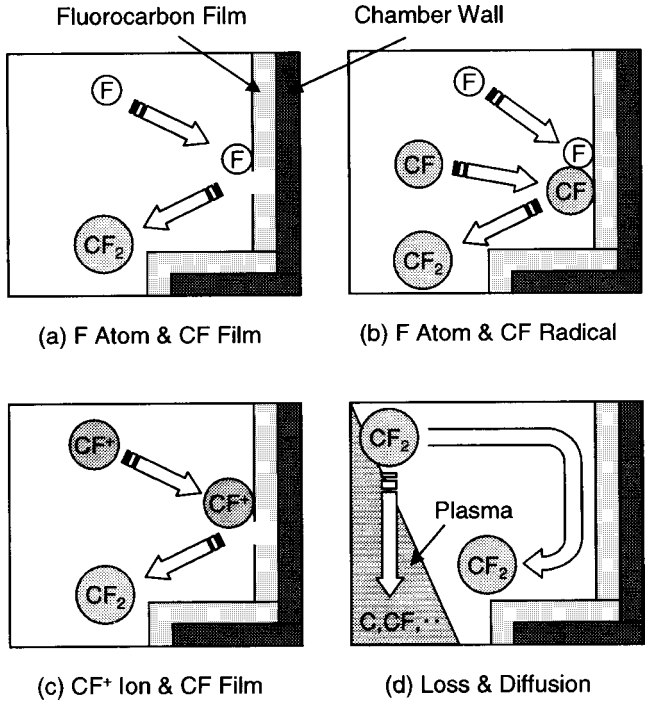

FIG. 3. Four models for formation of hollow CF_2 radical distribution; (a) etching reaction between F atoms and fluorocarbon films, (b) three-body association between CF radicals and F atoms, (c) sputtering of fluorocarbon film by CF_x^+ ions or neutralization of CF_x^+ ions, and (d) intensive loss in plasma region and diffusion of CF_2 radicals.

rescence wavelengths of the CF and CF_2 radicals are 255.2 $[A^2\Sigma^+(v'=0)\rightarrow X^2\Pi(v''=3)]$ and 271.0 $[\tilde{A}(0,2,0)\rightarrow\tilde{X}(0,2,0)]$ nm, respectively. The emission intensities of Ar* were measured in order to obtain information on the electron density and temperature in the plasma. X-ray photoelectron spectroscopy (XPS) was used to investigate the surface structure of fluorocarbon polymer deposited on the chamber wall.

III. RESULTS AND DISCUSSION

The spatial distribution of the line-averaged absolute CF_2 radical densities was measured by single-path IRLAS, and is shown in Fig. 2 as a function of microwave power. The distances of 0, 5, 10, and 21.5 cm shown in the figure correspond to beam paths reflected by mirrors 1, 2, 3, and 4, respectively, as shown in Fig. 1. A total pressure and a flow rate of C_4F_8 were 1.3 Pa and 60 sccm, respectively. The CF_2 radical density can be seen to decrease with increasing microwave power. Moreover, the CF_2 radical density has a hollow distribution; the density at the center of the wafer is lower than that in the vicinity of the chamber wall. At a microwave power of 1.0 kW, the CF_2 radical density was 1.1×10^{14} cm^{-3} and almost constant above the wafer. However, the density increased to 1.9×10^{14} cm^{-3} in the vicinity of the wall. From these results, it is considered that the C_4F_8 gas was depleted and the CF_2 radicals were thus dissociated into smaller species such as CF radicals, and C and F atoms due to electron impact even in the low microwave power region. Moreover, it has been reported that the self-sticking probability of CF_2 radicals increases by two orders of magnitude under ion bombardment.[9] This indicates that the loss of CF_2 radicals to the Si wafer is enhanced in the plasma region.

If CF_2 radicals are only generated in the plasma region through the dissociation of C_4F_8 gas, the radical densities should have either convex or uniform distribution. On the basis of the fact that the density is higher in the vicinity of the wall, we propose four models for the formation mechanism of this spatial distribution, as shown in Fig. 3. The first (a) is the generation of CF_2 radical via an etching reaction between F atoms and fluorocarbon films deposited on the chamber wall. The second (b) is via the three-body association between CF radicals and F atoms on the chamber wall. The third (c) is via the sputtering of fluorocarbon films with CF_x^+ ions or the neutralization of CF_x^+ ions on the chamber wall. The fourth (d) is due to the intensive loss of CF_2 radicals in the plasma region through electron-impact dissociation and sticking on the substrate[10] and the diffusion of CF_2 radicals from the ECR region in the upper part of plasma chamber toward the chamber wall.

In order to evaluate the first model, we modified the characteristics of the fluorocarbon films deposited on the chamber wall by O_2 or H_2 plasma pretreatment. The spatial distribution of the absolute CF_2 radical densities after H_2 or O_2 plasma treatment is shown in Fig. 4. The pretreatment conditions were total pressure of 1.3 Pa, microwave power of 1.0 kW, and H_2 (or O_2) gas flow rate of 60 sccm. The measurement of CF_2 radical density was carried out at a total pressure of 1.3 Pa, a microwave power of 1.0 kW, and a C_4F_8 gas flow rate of 40 sccm. By XPS it was confirmed that

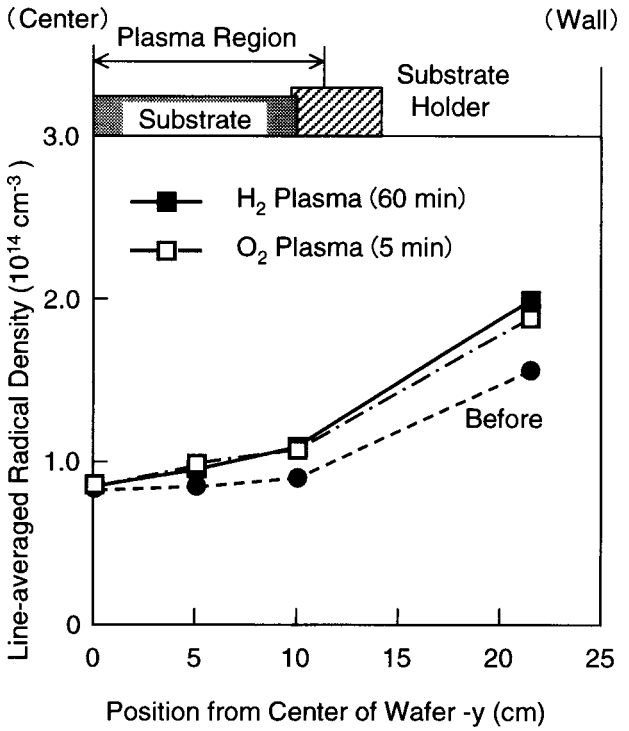

FIG. 4. Spatial distribution of the absolute CF_2 radical density after H_2 or O_2 plasma pretreatment.

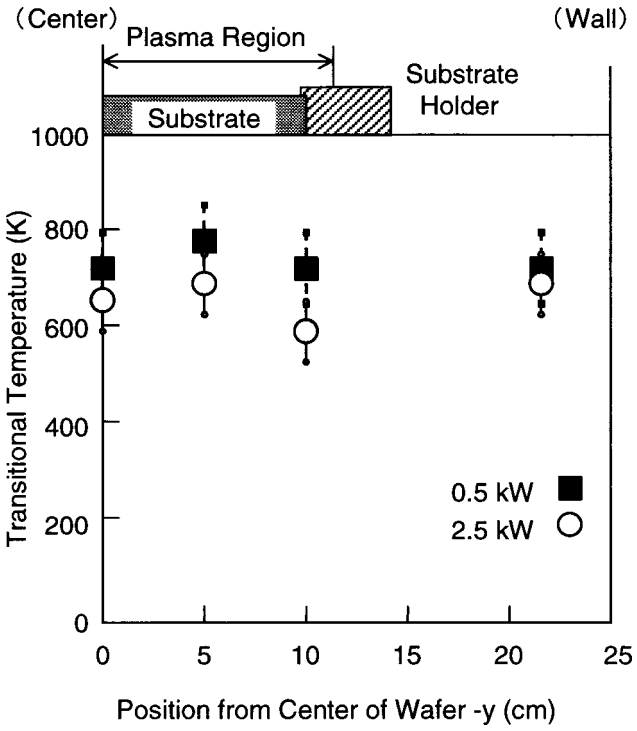

FIG. 5. Spatial distribution of the translational temperatures of CF_2 radicals as a function of microwave power.

the chemical structure of fluorocarbon films on the chamber wall became carbon-rich after both forms of pretreatment. The F/C ratios of the film surfaces were changed from 1.9 to 1.5 and 1.6 with H_2 and O_2 plasma treatment, respectively. It has been reported that the sticking probability of CF_x radicals to the wall decreases and the reaction probability between F atoms and films on the chamber wall decreases when the surface of films is carbon rich.[11] Therefore, the modification of film surfaces to the carbon-rich structure by H_2 or O_2 plasma treatment reduces the degree of radical generation from the chamber wall due to the reaction between F atoms and fluorocarbon films. It is found, however, that the CF_2 radical densities still increase in the vicinity of the wall after plasma pretreatment. This indicates that the generation of radicals by reaction between the films and F atoms is not the dominant mechanism for the increase in radicals in the vicinity of the wall. Therefore, the first model is inadequate.

The spatial distribution of the translational temperatures of CF_2 radicals is shown in Fig. 5 as a function of microwave power. The temperatures are estimated to be about 700 K. With this radical density distribution, where the CF_2 radical densities are much higher in the vicinity of wall, the measured temperature of CF_2 radicals is considered to be dominated by radical temperature outside the plasma region. If the radical generation by wall reaction is the primary factor in the formation of the hollow distribution, these radical temperatures should be almost the same as the chamber wall temperature of 400 K. The measured radical temperatures were higher than chamber wall ones by at least 300 K. This result discounts the validity of both the first and second models.

Next, we employed a combination of single-path IRLAS and LIF to clarify the mechanism of radical distributions.

The precise spatial distribution of the absolute CF_2 radical densities is shown in Fig. 6 as a function of microwave power. For all the following single-path IRLAS and LIF

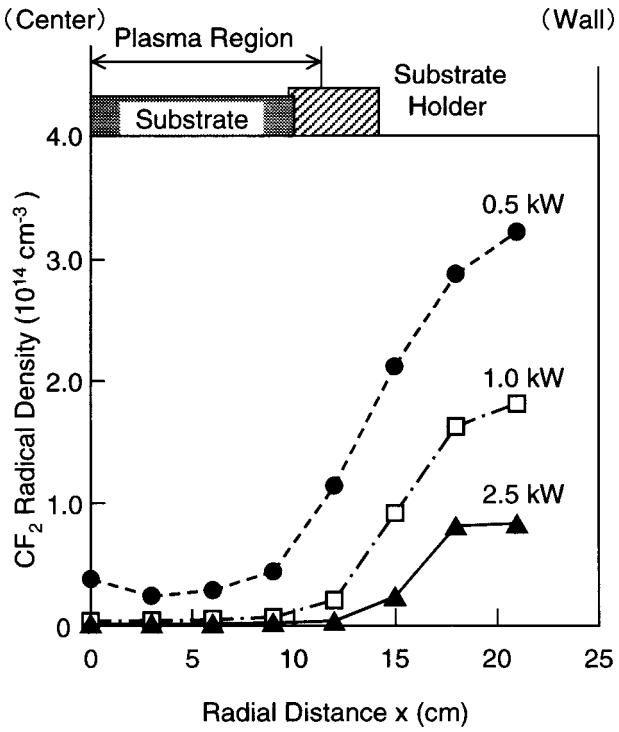

FIG. 6. Precise spatial distribution of the absolute CF_2 radical density as a function of microwave power.

measurements, the surfaces of the chamber walls and quartz windows were cleaned with O_2 plasma for 5 min before each measurement in order to remove the fluorocarbon films on the surfaces. The O_2 plasma cleaning was conducted at a microwave power of 1 kW, a total pressure of 1.3 Pa, and an O_2 gas flow rate of 60 sccm. The CF_2 radical densities were measured at a pressure of 1.3 Pa and a C_4F_8 flow rate of 60 sccm.

The CF_2 radical densities had a hollow distribution for every microwave power, and the overall density decreased with increasing microwave power in a similar manner to the results obtained with single-path IRLAS alone, as shown in Fig. 2. By using this method, it was clarified that the CF_2 radical density in the plasma region is clearly lower than outside the plasma region. The gradient of the CF_2 radical density toward the chamber wall was found to decrease with increasing microwave power. F atom and CF_x^+ ion generation in the plasma increases at higher microwave powers. Therefore, if the CF_2 radicals are formed via surface reactions, such as the first, second, and third models for a hollow distribution, the gradient in CF_2 radical density should be steepest near the wall. However, these models fail to explain why the CF_2 radical densities distributions flatten near the chamber wall, as observed clearly at 2.5 kW. The ion flux to the wall was measured by Langmuir probe and was found to of the order of $10^{12}\,cm^{-2}\,s^{-1}$ or below, which is considerably low. The flux of CF_2 radicals from the chamber wall was estimated to be of the order of $10^{17}\,cm^{-2}\,s^{-1}$ at a microwave power of 1.0 kW from the gradient in Fig. 6. Here, we have assumed that the diffusion coefficient of CF_2 radicals in the C_4F_8 plasma is $8.7\times10^3\,cm^2\,Pa\,s^{-1}$, which is the same as that of CF_2 radical in CF_4 plasmas. Thus, the radical flux is greater than the ion flux by over four orders of magnitude. These facts provide no support for the first, second, and third models.

The precise spatial distribution of the absolute CF_2 radical densities is shown in Fig. 7 as a function of pressure. The microwave power and C_4F_8 flow rate were 1.0 kW and 60 sccm, respectively. The CF_2 radical density distribution is hollow for all pressures, and the density increases with increasing pressure. At 4.0 Pa, the distribution of the CF_2 radical density is clearly flat near the chamber wall, which is a similar behavior to that at a microwave power of 2.5 kW, as shown in Fig. 6. The flux of CF_2 radicals near the chamber wall is lower than that in the plasma boundary region. The hollow distribution is considered to be a result of radical loss processes in the plasma region rather due to radical generation at the chamber wall. Therefore, the fourth model, as shown in Fig. 3(d), is supported by these results.

The precise spatial distribution of the absolute CF radical densities is shown in Fig. 8 as a function of microwave power. The plasma was generated at a C_4F_8 flow rate of 60 sccm and under a pressure of 1.3 Pa. The absolute density of CF radicals in the plasma region is on the order of $10^{13}\,cm^{-3}$ and higher than that of CF_2 radicals. Outside the plasma region, however, the absolute density of CF radical density is lower than that of CF_2 radicals. It is noteworthy that the spatial distributions at 0.5 and 1.0 kW have maximums near the boundary of the plasma region. This can be explained as

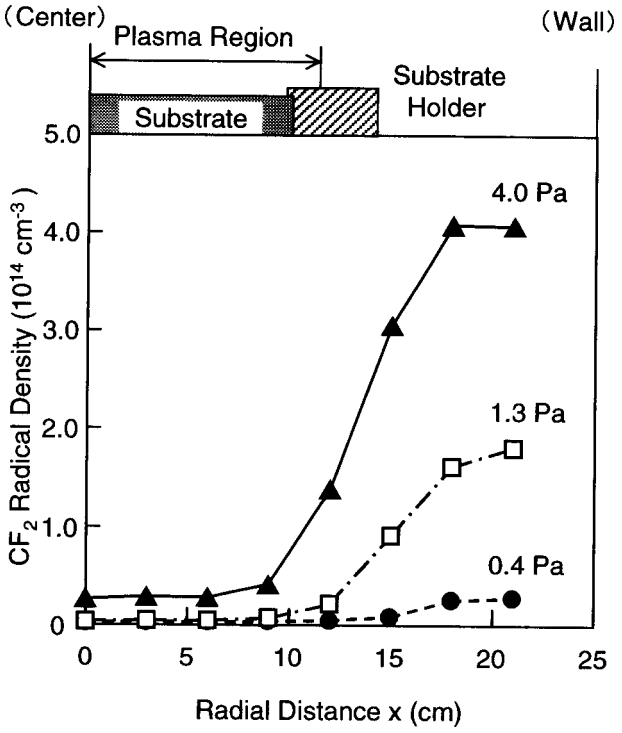

FIG. 7. Precise spatial distribution of the absolute CF_2 radical density as a function of pressure.

follows: It has been reported that CF radicals are generated from CF_2 radicals by electron-impact dissociation when the CF_2 radical density is much higher than that of CF radicals.[10,12] Therefore, in this study, at 0.5 and 1.0 kW microwave power, CF radicals are considered to be generated

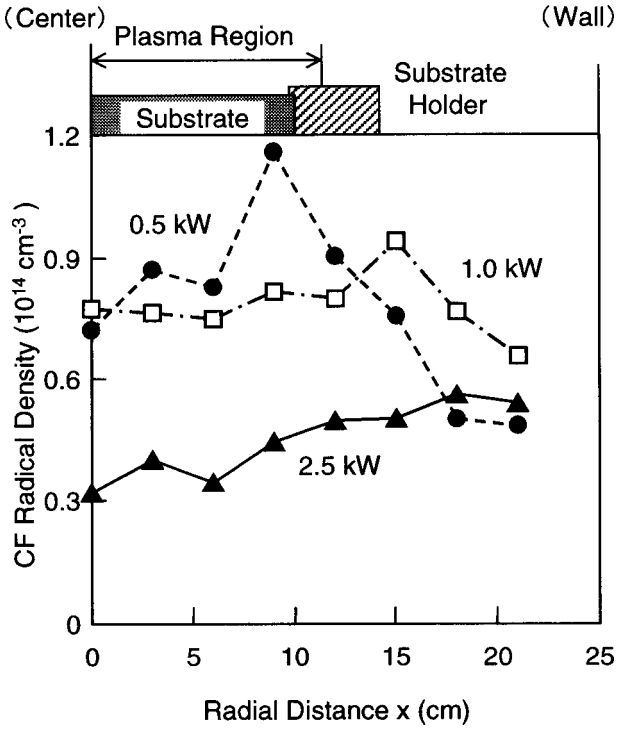

FIG. 8. Precise spatial distribution of the absolute CF radical density as a function of microwave power.

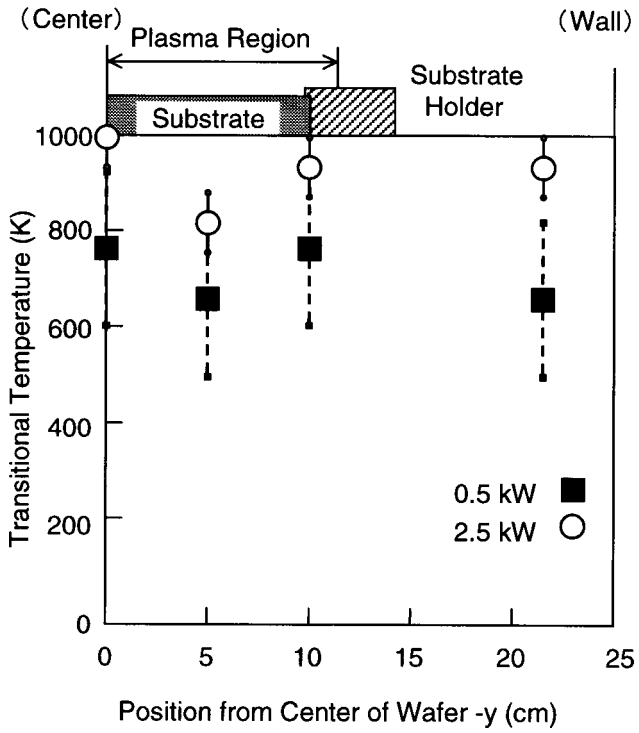

FIG. 9. Spatial distribution of the translational temperatures of CF radicals as a function of microwave power.

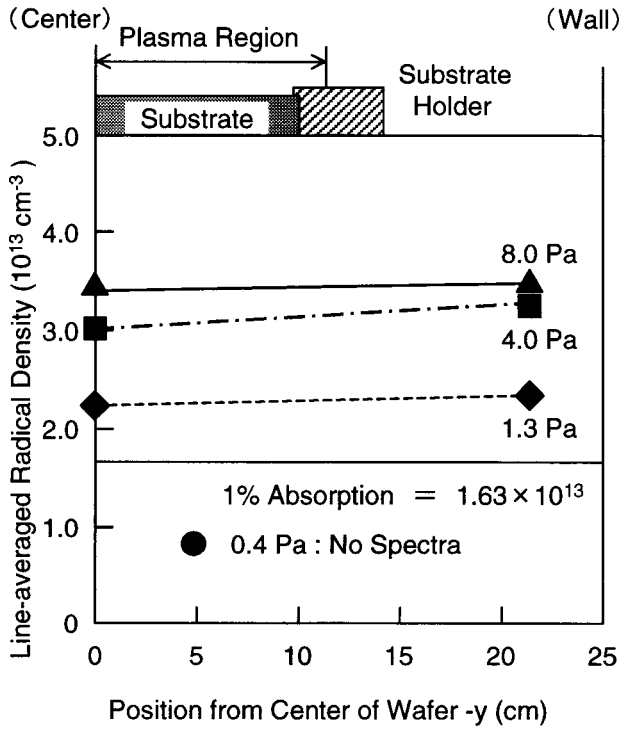

FIG. 10. Spatial distribution of the absolute CF_3 radical density as a function of pressure.

from the electron-impact dissociation of CF_2 radicals in the plasma region. As CF_2 radicals diffuse into the plasma region, as shown in Fig. 6, CF radicals are primarily generated near the plasma boundary region. Therefore, the generated CF radicals are considered to diffuse toward the center of the plasma region, and toward the chamber wall from the plasma boundary region. CF radicals are lost at the wall because the sticking coefficient of CF radicals is relatively high,[13] resulting in a decrease in CF radical density in the vicinity of the wall.

At 2.5 kW, however, the CF radical density has the hollow distribution. As there is almost no diffusion of CF_2 radicals into the plasma under these conditions, as shown in Fig. 6, the generation of CF radicals near the plasma boundary is considered to become negligible. As a model for the hollow distribution, it is considered that the C and F atoms diffuse toward the wall where they recombine to form CF radicals. This is suggested from the fact that CF radicals dissociate into C and F atoms in the plasma region. The spatial distribution of translational temperatures of the CF radicals is shown in Fig. 9. The translational temperature was estimated to be about 700 K near the chamber wall, which is as high as that of the CF_2 radicals. This indicates that the CF radical generation at the chamber wall is small. Therefore, at high microwave power, CF radical generation is considered to be high at the ECR point, from which the radicals diffuse toward the chamber wall. This mechanism is similar to the suggested formation mechanism of the CF_2 radical distribution.

The spatial distribution of the absolute CF_3 radical density is shown in Fig. 10 as a function of pressure. The microwave power and C_4F_8 flow rate were 1.5 kW and 90 sccm, respectively. The CF_3 radical density increased with increasing pressure. The CF_3 radicals at the center of wafer can be seen to have almost the same density as in the vicinity of the chamber wall at all pressures. These results indicate that there is no generation of CF_3 radical from the chamber wall and no diffusion from the upper part of the chamber, in contrast to CF and CF_2 radicals. Moreover, the sticking coefficient of CF_3 radicals is considered to be very low. Therefore, CF_3 radicals are suggested to be generated via surface reactions on the wafer in the plasma region, which is consistent with results reported previously.[14]

IV. CONCLUSION

The precise spatial distribution of the absolute CF_x radical density and the translational temperatures parallel to the wafer have been measured for ECR–C_4F_8 plasma by single-path IRLAS combined with LIF using identical beam paths. It is found that the CF radical density is higher than that of CF_2 radicals in the plasma region and lower outside the plasma region. The CF_2 radical density always exhibits a hollow distribution, and the gradients of the distribution flatten near the chamber wall. The spatial distribution of the CF_2 radicals is formed by the electron-impact dissociation of C_4F_8 and diffusion from the upper part of the plasma chamber toward the chamber wall. CF radicals are generated via the electron-impact dissociation of CF_2 radicals and diffuse into the plasma region. CF_3 radicals are generated from surface reaction on the wafer in the plasma region, which is a considerably different behavior to either CF or CF_2 radicals.

These results are of vital importance for understanding radical behaviors in etching and CVD processes using fluo-

rocarbon plasmas and offer fundamental information for the development of equipment with increased production levels.

ACKNOWLEDGMENTS

The authors would like to thank Professor A. Kono of the Nagoya University, Dr. J. Hata, Dr. T. Ohta, and K. Hama of Tokyo Electron Ltd., and Y. Uchida of Mechanitron for their useful advice and cooperation. This work was supported by a Grant-in-Aid for Scientific Research from the Ministry of Education, Science, Sports, and Culture, Japan.

[1] K. Endo and T. Tatsumi, Appl. Phys. Lett. **68**, 2864 (1996).
[2] K. Takahashi, M. Hori, and T. Goto, J. Vac. Sci. Technol. A **14**, 2011 (1996).
[3] S. Hayashi, H. Nakagawa, M. Yamanaka, and M. Kubota, Jpn. J. Appl. Phys., Part 1 **36**, 4845 (1997).
[4] K. Maruyama, K. Ohkouchi, Y. Ohtsu, and T. Goto, Jpn. J. Appl. Phys., Part 1 **33**, 4298 (1994).
[5] K. Takahashi, M. Hori, and T. Goto, J. Vac. Sci. Technol. A **14**, 2004 (1996).
[6] K. Miyata, K. Takahashi, S. Kishimoto, M. Hori, and T. Goto, Jpn. J. Appl. Phys., Part 2 **34**, L444 (1995).
[7] P. B. Davies, P. A. Hamilton, J. M. Elliott, and M. J. Rice, J. Mol. Spectrosc. **102**, 193 (1983).
[8] C. Suzuki, K. Sasaki, and K. Kadota, J. Appl. Phys. **82**, 5321 (1997).
[9] K. Takahashi, M. Hori, M. Inayoshi, and T. Goto, Jpn. J. Appl. Phys., Part 1 **35**, 3635 (1996).
[10] K. Takahashi, M. Hori, and T. Goto, Jpn. J. Appl. Phys., Part 1 **33**, 4745 (1994).
[11] Y. Horiike, K. Kubota, H. Shindo, and T. Fukasawa, J. Vac. Sci. Technol. A **13**, 801 (1995).
[12] S. Den, P. O'Keeffe, Y. Hayashi, M. Ito, M. Hori, and T. Goto, Jpn. J. Appl. Phys., Part 1 **36**, 4588 (1997).
[13] K. Miyata, M. Hori, and T. Goto, Jpn. J. Appl. Phys., Part 1 **36**, 5340 (1997).
[14] K. Miyata, M. Hori, and T. Goto, J. Vac. Sci. Technol. A **14**, 2083 (1995).